Universiteit Leiden
The Netherlands

Newts in time and space: the evolutionary history of Triturus newts at different temporal and spatial scales
Espregueria Themudo, G.

CHAPTER 6

CURRENT GENE FLOW ACROSS A NEWT HYBRID ZONE FOLLOWS LOCAL
ECOLOGICAL CONDITIONS

G. Espregueira Themudo[1,2] and J. W. Arntzen[1]

[1] *National Museum of Natural History, P. O. Box 9517, 2300 RA Leiden, The Netherlands.*
[2] *CIBIO, Centro de Investigação em Biodiversidade e Recursos Genéticos, Campus Agrário de Vairão, 4485-661*
Vairão, Portugal.

Contents

Manuscript in preparation

Abstract

Conditions of the environment can influence the number of genes that pass through an interspecific hybrid zone. In long hybrid zones, different patterns may emerge depending on local conditions. We studied gene flow across a ca. 500 km long hybrid zone between two newt species, *Triturus marmoratus* and *T. pygmaeus,* in the Iberian Peninsula. We sequenced one mitochondrial and three nuclear genes in 355 individuals from 73 populations to test *a priori* hypotheses on the level and symmetry of gene flow, under an *Isolation with Migration* framework. Four different environmental settings associated with the position and structure of the hybrid zone (identified with ecogeographical modeling; Arntzen & Espregueira Themudo, J. Biogeogr. 35, 2008) included i) a lowland - mountain transition at Sierra de Gata in western Spain and ii) the river Tejo in central Portugal forming a wide and a narrow barrier to gene flow, respectively. In between Tejo and Gata (iii) the position of the zone is determined by a minimum spanning distance with no environmental signature, as predicted by hybrid zone theory. The Portuguese coastal area (iv) has been subject to the rapid expansion of one of the species (*T. pygmaeus*) over the other, following edaphic and climatological features of the environment. There we observed a unidirectional pattern of gene flow and symmetry elsewhere. The prediction that gene flow across a barrier (Tejo river) would be lower than in an area without such a barrier was not confirmed. However, a temporal analysis indicated that most local gene flow is ancient, indicating that the barrier is stronger at present then it was in the past.

Introduction

Closely related species may 'meet, mate and produce hybrids' (Barton and Hewitt, 1985), forming more or less narrow hybrid zones that can span for hundreds of kilometers. The study of these areas of limited intergradation has provided new insights into the process of speciation (Coyne and Orr, 2004). Across the hybrid zone populations will have progressively fewer genotypes of the first species until only pure genotypes of the second species are found, forming a cline of variable width and shape. The width of the cline depends on the balance of two opposing forces: dispersal of parental individuals into the hybrid zone and endogenous selection against hybrids, caused by the disruption of intra-genomic coadaptation. This clinal model is also referred to as the 'tension zone' model (a term coined by Key, 1969). In strict tension zones, the frequency of alternative genotypes in a population is only dependent to the distance to the centre of the hybrid zone (Barton, 1979; Szymura and Barton, 1986).

On another extreme, the 'mosaic' model of hybrid zones postulates that two species will be distributed according to habitat preference, and distance to the centre of the zone is not a good predictor for the proportion of parental genotypes in a population (Rand and Harrison, 1989). Mosaic hybrid zones are usually bimodal hybrid zones, with a low percentage of hybrid genotypes (Jiggins and Mallet, 2000). The two models can be seen as part of a continuum, and can be observed in the same system, dependent on spatial scale (Arntzen, 1996). Indeed, the position of a clinal hybrid zone may be determined by the distribution of landscape elements and the presence of geographical barriers, such as altitude (or perhaps relief) in the fire-bellied toads, *Bombina bombina / B. variegata*, hybrid zone (Arntzen, 1978), or the Strait of Gibraltar in the long-eared bats, *Myotis myotis / M. punicus*, hybrid zone (Castella et al., 2000).

Width and shape of the clinal hybrid zone may be affected by smaller landscape elements, such as forestation, the availability of a particular breeding habitat, or the distribution of relief (e.g. KRUUK et al., 1999; SZYMURA, 1988) or different degrees of complexity of the habitat (MACCALLUM *et al*., 1998; YANCHUKOV *et al.*, 2006). Hybrid zones are not necessarily stable neither (ARNTZEN and WALLIS, 1991; BRITCH *et al.,* 2001; FITZPATRICK et al., 2004). Changes in the environment can favor one of the species, allowing it to expand into the area and

eventually supersede the other species (ARNTZEN, 1978; ARNTZEN and WALLIS, 1991; DASMAHAPATRA *et al.*, 2002; PEARSON, 2000).

Large rivers and mountain ranges may pose barriers to amphibian dispersal. Evidence supporting this notion is mostly derived from the analysis of distribution patterns in which the edge of the range coincides with the feature considered (GASCON, 1996; GARCÍA-PARÍS *et al.*, 1998). Alternatively, phylogeographic patterns may coincide with intraspecific genetic differentiation, such as the Mondego river in central Portugal, that was implicated in the maintenance of a hybrid zone in the salamander *Chioglossa l. lusitanica* and *C. l. longipes* (ALEXANDRINO *et al.*, 2000). Once crossed, obviously, neither a river nor a mountain range will form a barrier any longer. In terms of their barrier function, the essential difference between a mountain range and a river is in their width. Considering its limited width, a river is best qualified as a semi-permeable barrier, the strength of which will depend on the swimming and survival capability of the species during its various life-stages.

In long hybrid zones, environmental conditions may be specific to a part of the system, like differences in land use. These different conditions may produce opposing patterns in separate areas of the hybrid zone, such as in the *Mus musculus* hybrid zone in the Czech Republic and Germany, where introgression went in opposite directions (Božíková et al., 2005). The analysis of species distributions as a function of the environment gives, in parapatrically distributed and hybridizing species, rise to testable hypothesis in the amount of gene flow they exhibit. We here study the amount of gene flow across a bimodal hybrid zone of two species of newts in the Iberian Peninsula. We have a good overall picture of how the environment regulates the distribution of the species (Chapter 8), with detailed ecogeographical models for the entire hybrid zone. This zone is particularly well-suited for such an approach, because it is long (ca. 500 km), with various environmental settings determining its position (soil type, river, mountains). We here focus on areas where interspecific interactions are subject to clearly different ecogeographical signatures (CHAPTER 8) and we, thus, expect the genetic interaction of the species to vary with space.

Triturus marmoratus and *T. pygmaeus* are two European newt species (although sometimes still referred to as subspecies, LOUREIRO *et al.*, 2008) with a parapatric distribution. The contact zone runs along an east-west axis from Madrid in Spain to Abrantes in Portugal, where the zone bends northwards, with *T. pygmaeus*

present in the south and along the Atlantic coast up to Aveiro and *T. marmoratus* inland and to the north (Figure 1). Southwest of the bend, we observed a residual population of *T. marmoratus* (CHAPTER 9). Since the population is entirely surrounded by *T. pygmaeus* it effectively constitutes an enclave. A detailed study in the area revealed a single possible hybrid among ca. 400 individuals studied (Chapter 9). North of here, about 150 km of dune habitat is occupied by *T. pygmaeus* (Fig. 1, area A; 'windows 1-13' in Chapter 8). It is important to note that *T. marmoratus* is widely distributed in the coastal dunes north of Aveiro. The presence of an enclave, the near absence of interspecific hybridization and the remarkable distribution pattern along the coast, suggests the fast advance of *T. pygmaeus* up to the Vouga estuary in Aveiro, while superseding *T. marmoratus*. We predict that gene flow is absent or very limited and when it occurs, unidirectional from the advancing species, *T. pygmaeus* into the receding species, *T. marmoratus*,and localized at the edge of the wave of advance.

On the opposite side of joint *T. marmoratus – T. pygmaeus* distribution at the eastern fringe of the Central System, the contact zone appears residual (sensu SZYMURA, 1993) with a low density of populations and no documented hybridization (GARCÍA-PARÍS et al., 2001). However, a dense network of populations spanning both species was found at the Sierra de Gata mountains, at the western fringe of the Central System (Figure 1, area D). The species divide is positioned along the southern mountain slopes and is fairly abrupt. Locally it is difficult to disentangle between the multiple climatological parameters that coincide with the species border (CHAPTER 8). Because of the barrier function of (or associated with) the mountain/lowland transition, our prediction here is that the hybrid zone is stable with little or no interspecific gene flow. Note however that the genetic data on the Gata transect are as yet incomplete.

In central Portugal, at the Tejo Basin east of Abrantes (Figure 1, area B), the position of the hybrid zone coincides with the river, that seems to be working as a barrier to dispersal (Chapter 8; 'windows 14-20'). We predict that local gene flow will be low, given the presence of the barrier (but not as low as at the mountains) and symmetrical as there is no evidence for large scale movement of the parapatric range border.

Finally, around Idanha-a-Nova, in eastern Portugal (Figure 1, area C), the position of the contact zone appears not associated with features of the environment

(Chapter 8; 'windows 21-26'). Rather, the position of the zone seems to be dependent on fixed points to the west (B) and east (D). Following tension zone theory (BARTON and HEWITT, 1985), the situation in Idanha (C) represents a minimum-spanning distance between the Tejo river and the Gata mountains. Because stable at either side, at Idanha the zone will be moving neither, yielding the prediction of gene-flow symmetry. Because of the absence of a physical barrier to dispersal, we predict that gene flow across the zone will be relatively high. Our predictions are summarized in Table 1.

Table 1- Hypothesis regarding symmetry in gene flow ($2N_1m_1=2N_2m_2$), presence of gene flow from *Triturus pygmaeus* to *T. marmoratus* ($2N_1m_1>0$) and in the opposite direction ($2N_2m_2>0$). The predicted level of gene-flow is $D < B < A < C$.

Area	$2N_1m_1=2N_2m_2$	$2N_1m_1>0$	$2N_2m_2>0$
A - Coast	no	yes	no
B - Tejo	yes	yes	yes
C - Idanha	yes	yes	yes
D - Gata	not applicable	no	no

Material and methods

<u>Sampling</u>

We sampled 355 marbled newts in 73 populations across the range of both species in Portugal, Spain and France between 1998 and 2008 (DNA protocol

DNA extraction followed standard protocols from the DNeasy extraction kit (Qiagen). The three introns examined were: □-Fibrinogen intron 7 (□fibint7), Calreticulin intron

C (CalintC), and Platelet-derived growth factor receptor □ (Pdgfr□) intron 11 (Chapter 3). We also examined the mitochondrial gene NADH dehydrogenase subunits 4 (ND4). PCR conditions consisted of a denaturation step at 94 ºC for 4 minutes, followed by 35 cycles of a denaturing step (30'' at 94 ºC), an annealing step (45'' at 57-68 ºC depending on the fragment) and an extension step (90'' at 72 ºC) with a final extension of 4' at 72 ºC. The primers used are presented in Chapter 3. Reaction chemistry was 23 μL of H2O, 3 μL of buffer (15 μM MgCl2), 1.8 μL of 25 μM $MgCl_2$, 0.6 μL of dNTPs (10 mM), 0.2 μL of each primer (100 μM) and 0.2 μL (1 U) of Taq DNA Polymerase (Qiagen). Sequences were obtained commercially at

Macrogen Inc (Seoul, Korea). Both DNA strands were sequenced to increase the accuracy of the results.

Sequence analysis

DNA sequences were edited using Chromas (Technelysium Pty Ltd.) to check for basecalling errors. Insertion/deletion polymorphisms (indels) reflecting heterozygosity were reconstructed by hand through sequence comparison with a homozygous individual. Sequences polymorphic for indels were identified based on the presence of overlapping peaks downstream from particular areas of the sequence, using both forward and reverse primers. Individual alleles were inferred with the software Phase (STEPHENS *et al.*, 2001). The obtained sequences were aligned in BioEdit (HALL, 1999). Multi-base indels were pruned leaving the first base and any polymorphic bases, to avoid overestimating the differences between haplotypes. Nucleotide base composition, the transition–transversion ratio and the percentage sequence divergence (p-distance) were calculated with MEGA4 software (TAMURA *et al.*, 2007). Translating the coding regions of the sequences to amino acids did not reveal any unexpected stop codons. We calculated haplotype diversity (h), nucleotide diversity (π), and Watterson's θ for both species using DNAsp (ROZAS *et al.*, 2003).

Table 1; Figure 1). Adult newts and larvae were captured using dip nets under the appropriate licences from 'Instituto da Conservação da Natureza' (Portugal), 'Consejarias del Medio Ambiente' (Spain) and 'Ministére de l'Environment' (France). Adults were identified based on morphology, and larvae were identified by allozymes (see CHAPTERS 7 and 9). To preserve the DNA, samples were immediately stored in liquid nitrogen and later transferred to a -80º C freezer.
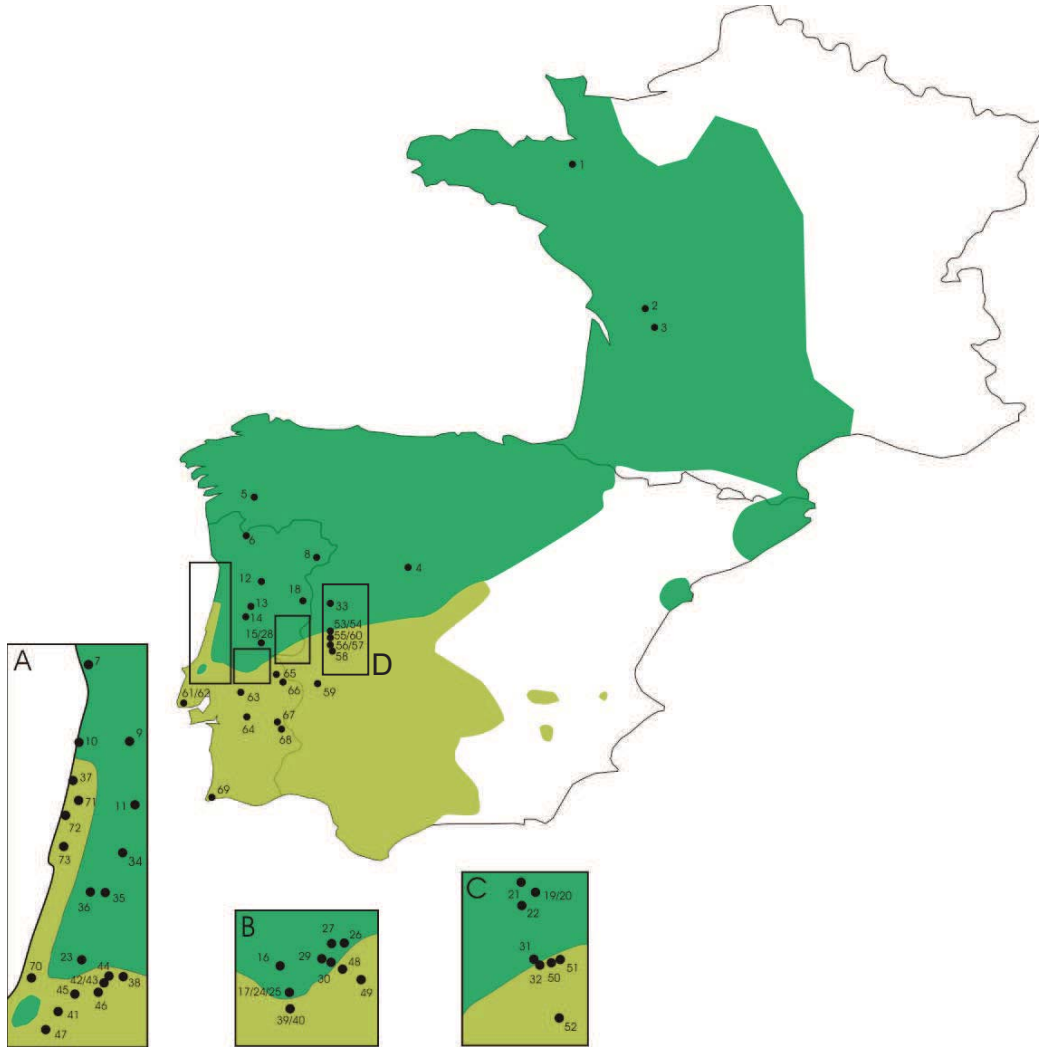

Figure 1 - Distribution map showing the range of *Triturus marmoratus* (in dark green) and *T. pygmaeus* (in light green) in Western Europe. Black dots represent sampling localities. Boxes labelled from A to C indicate areas sampled in more detail (see text). A – Coastal area, B – Tejo basin, C – Idanha-a-Nova and D - Sierra da Gata.

DNA protocol

DNA extraction followed standard protocols from the DNeasy extraction kit (Qiagen). The three introns examined were: β-Fibrinogen intron 7 (βfib*int*7), Calreticulin intron C (Cal*int*C), and Platelet-derived growth factor receptor α (Pdgfrα) intron 11 (CHAPTER 3). We also examined the mitochondrial gene NADH dehydrogenase subunits 4 (ND4). PCR conditions consisted of a denaturation step at 94 ºC for 4 minutes, followed by 35 cycles of a denaturing step (30'' at 94 ºC), an annealing step (45'' at 57-68 ºC depending on the fragment) and an extension step (90'' at 72 ºC) with a final extension of 4' at 72 ºC. The primers used are presented in CHAPTER 3. Reaction chemistry was 23 µL of H_2O, 3 µL of buffer (15 µM $MgCl_2$), 1.8 µL of 25 µM $MgCl_2$, 0.6 µL of dNTPs (10 mM), 0.2 µL of each primer (100 µM) and 0.2 µL (1 U) of Taq DNA Polymerase (Qiagen). Sequences were obtained commercially at Macrogen Inc (Seoul, Korea). Both DNA strands were sequenced to increase the accuracy of the results.

Sequence analysis

DNA sequences were edited using Chromas (Technelysium Pty Ltd.) to check for basecalling errors. Insertion/deletion polymorphisms (indels) reflecting heterozygosity were reconstructed by hand through sequence comparison with a homozygous individual. Sequences polymorphic for indels were identified based on the presence of overlapping peaks downstream from particular areas of the sequence, using both forward and reverse primers. Individual alleles were inferred with the software Phase (STEPHENS *et al.*, 2001). The obtained sequences were aligned in BioEdit (HALL, 1999). Multi-base indels were pruned leaving the first base and any polymorphic bases, to avoid overestimating the differences between haplotypes. Nucleotide base composition, the transition–transversion ratio and the percentage sequence divergence (p-distance) were calculated with MEGA4 software (TAMURA *et al.*, 2007). Translating the coding regions of the sequences to amino acids did not reveal any unexpected stop codons. We calculated haplotype diversity (h), nucleotide diversity (π), and Watterson's θ for both species using DNAsp (ROZAS *et al.*, 2003).

Table 1- List of sample localities per species with information on the country (F=France, S=Spain, P=Portugal), geographical coordinates and sample size (N) for three nuclear and one mitochondrial genes. Top panel *Triturus marmoratus* and bottom panel *T. pygmaeus.*

Triturus marmoratus Locality	Population	Country	Latitude (N)	Longitude (W)	βfib*int*7	Cal*intC*	Pdgfrα	mtDNA
Mayenne	1	F	48º 17' 60"	0° 37' 01"	4	4	4	
Confolens	2	F	46º 01' 00"	- 0º 40' 00"		1	1	
Rochechouart	3	F	45º 49' 00"	- 0º 50' 00"		3	3	
El Berrueco	4	S	40º 54' 00"	3º 53' 00"		3	4	
Cabreiras	5	S	42º 26' 49"	7º 54' 20"	4	5	4	5
Serra do Gerês	6	P	41º 49' 04"	8º 02' 12"	4	5	7	5
Porto	7	P	41º 09' 12"	8º 38' 31"	5	5	5	5
Mogadouro	8	P	41º 20' 48"	6º 36' 33"	5	5	5	5
Nespereira de Baixo	9	P	40º 45' 58"	8º 22' 19"	5	5	5	5
Torreira	10	P	40º 45' 51"	8º 42' 34"	2	3	3	3
Saide	11	P	40º 27' 02"	8º 19' 40"	2	2	2	5
Mezio	12	P	40º 56' 31"	7º 48' 43"	1	5	5	5
Nelas	13	P	40º 29' 30"	7º 50' 36"	5	5	5	10
Madeirã	14	P	39º 56' 38"	8º 02' 24"				5
Pedra do Altar	15	P	39º 42' 37"	7º 49' 14"				4
Santos	16	P	39º 36' 03"	7º 57' 45"	5	4	4	5
Domingos da Vinha	17	P	39º 31' 24"	7º 56' 48"				5
Castelo Mendo	18	P	40º 35' 15"	6º 56' 38"	3	3	4	5
Monte do Conde	19	P	40º 10' 08"	7º 15' 00"				3
Aldeia de João Pires	20	P	40º 06' 48"	7º 08' 45"				3
São João do Deserto	21	P	40º 08' 28"	7º 11' 31"	5	4	5	5
Aldeia Stª Margarida	22	P	40º 03' 08"	7º 15' 53"				5
Santa Catarina	23	P	39º 27' 02"	9º 00' 54"	3	4	4	4
Areia 2	24	P	39º 30' 50"	7º 55' 54"	4	5	5	5
Areia 3	25	P	39º 30' 50"	7º 56' 02"				5
Vila Velha de Ródão	26	P	39º 40' 12"	7º 40' 06"	4	4	5	4
Vilar de Boi	27	P	39º 40' 18"	7º 44' 12"	5	5	5	5
Vale da Figueira	28	P	39º 40' 52"	7º 44' 50"				5
Carepa	29	P	39º 37' 33"	7º 46' 23"	5	5	5	5
Fratel	30	P	39º 37' 06"	7º 44' 18"	5	5	5	5
Idanha-a-Nova	31	P	39º 56' 02"	7º 11' 51"	5	5	5	4
Senhora do Almurtão	32	P	39º 54' 23"	7º 09' 55"	4	5	5	5
Serradilla del Llano	33	S	40º 29' 39"	6º 20' 42"	5	5	5	5
Coimbra	34	P	40º 12' 28"	8º 24' 44"				5
Sicó	35	P	40º 01' 09"	8º 31' 52"				5
	36	P	40º 01' 10"	8º 37' 30"				10

Table 1 (cont.)

Triturus pygmaeus Locality	Population	Country	Latitude (N)	Longitude (W)	βfib*int7*	Cal*intC*	Pdgfrα	mtDNA
Praia de Vagueira	37	P	40º 34' 32"	8º 45' 23"	10	10	10	10
Tomar	38	P	39º 36' 15"	8º 25' 03"	5	5	5	5
Gavião 1	39	P	39º 28' 36"	7º 56' 19"	3	5	6	8
Gavião 2	40	P	39º 27' 32"	7º 55' 55"				5
Mosteiro Alcanene	41	P	39° 25' 47"	8º 50' 26"	4	4	4	
Rexaldia 1	42	P	39º 34' 40"	8º 32' 03"	1	1	1	1
Rexaldia 2	43	P	39º 34' 38"	8º 31' 59"	2	3	4	4
Assentiz - Fungalvaz	44	P	39º 35' 44"	8º 30' 39"	5	5	5	5
Serra de Stº António	45	P	39º 30' 55"	8º 43' 44"	5	5	5	5
Alqueidão	46	P	39º 32' 17"	8º 34' 51"	1	5	5	5
Rio Maior	47	P	39º 20' 46"	8º 54' 55"	5	5	5	6
Velada	48	P	39º 34' 49"	7º 42' 04"	5	5	2	5
Nisa	49	P	39º 33' 01"	7º 35' 34"	1	1	1	5
Zebreira West	50	P	39º 50' 32"	7º 06' 59"	5	5	5	5
Zebreira	51	P	39º 55' 56"	7º 05' 32"	2	3	4	4
Rosmaninhal	52	P	39º 45' 08"	7º 05' 50"	5	5	5	5
Casar de Palomero 1	53	S	40° 16' 44"	6° 14' 17"	4	4	4	5
Casar de Palomero 2	54	S	40° 16' 32"	6° 14' 27"	1	1	1	
Palomero	55	S	40º 15' 02"	6º 19' 51"	5	5	5	5
El Bronco	56	S	40º 12' 52"	6º 19' 56"	5	5	5	5
Stª Cruz de Paniagua	57	S	40º 11' 48"	6º 19' 59"	3	4	4	5
Aceitunas	58	S	40º 09' 05"	6º 19' 23"	4	4	4	4
Alcuescar	59	S	39º 05' 21"	6º 21' 49"	4	5	5	5
Pedro Muñoz 3	60	S	40º 15' 32"	6º 20' 46"	1	1	1	4
Sintra 1	61	P	38º 47' 38"	9º 25' 33"	3	3	2	2
Sintra 2	62	P	38º 47' 16"	9º 23' 17"	5	5	5	4
Mora	63	P	38º 57' 46"	8º 08' 45"	4	5	4	4
Mitra	64	P	38º 32' 17"	8º 00' 06"	5	5	5	5
Esperança	65	P	39º 10' 05"	7º 10' 57"	7	9	10	8
Sovrete	66	P	39º 16' 07"	7º 17' 03"				3
Mourão	67	P	38º 24' 47"	7º 18' 58"	2	1	1	2
Granja	68	P	38º 17' 59"	7º 15' 18"	5	4	4	5
Vila do Bispo	69	P	37º 04' 56"	8º 54' 35"	4	5	5	5
Valado dos Frades	70	P	39º 35' 51"	9º 00' 33"				5
Calvão	71	P	40º 28' 13"	8º 42' 18"				3
Mira	72	P	40º 23' 54"	8º 47' 16"				4
Quiaios	73	P	40º 14' 42"	8º 48' 00"				4

To represent relationships between haplotypes, we built phylogenetic networks for each gene, using the Median Joining algorithm as implemented in the program Network (BANDELT *et al.*, 1999). For intraspecific data, polymorphism is scarce and relationships between alleles may not be hierarchical, so networks will display the information from these genes more adequately than trees (POSADA and CRANDALL, 2001).

Mutation and recombination rates for IM analysis

In the absence of estimates on the mutation rates of the nuclear genes here analyzed, they were estimated with Beast 1.4.8 (DRUMMOND and RAMBAUT, 2007), under a strict clock model, HKY substitution model and a normal prior on the separation of *T. cristatus / T. marmoratus* with a mean of 24 Ma (millions of years), following (STEINFARTZ *et al.*, 2007). We then calculated the geometric mean of mutation rates, and mutation rate per generation by multiplying the per year rate with generation time. Since generation times vary geographically from 1-4 years in *T. pygmaeus* (CAETANO and CASTANET, 1993; DIAZ-PANÍAGUA, 1996) and 2-6 years in *T. marmoratus* (JEHLE *et al.*, 2001; CAETANO and CASTANET, 1993; JAKOB *et al.*, 2003; FRANCILLON-Vieillot, 1990), we accepted a generation time of 4 years, by excluding the population used in Diaz-Paníagua (1996) that is aberrantly small-sized compared to other populations of *T. pygmaeus*. Mutation rates and generation time are required to convert model parameter estimates from IMa (see below) into demographic quantities of number of migrants, effective population sizes and time of cladogenesis.

Isolation with Migration (IM) analyses assumes the absence of intralocus recombination. We tested this assumption by calculating the Φ_w statistic with PhiPack (BRUEN *et al.*, 2006). This statistic was less sensitive in simulation studies to mutation rate correlation than other similar statistics in simulation studies, making it less prone to falsely infer recombination when levels of homoplasy are high. PhiPack calculates *P*-values under the null hypothesis of no recombination. We used both available methods in the software to obtain these *P*-values: the analytical approach and a permutation test with 1000 permutations.

<u>IM analysis</u>

We carried out estimations of demographic parameters and dispersal rates with the coalescent based program IMa (HEY and NIELSEN, 2004) on three datasets from: the coastal area of Portugal, the Tejo basin in central Portugal, and the Idanha-a-Nova region close to the Spanish border (see areas A, B and C in Figure 1).

To determine appropriate parameter priors, we ran some initial runs with large priors for all the parameters, under the HKY substitution model. Runs started with 10,000 burnin steps after which they were allowed to continue until the minimum effective sample size (ESS) was >100. The Isolation with Migration (IM) model (Nielsen and Wakeley, 2001) assumes that two populations (or species) diverged from one ancestral populations at a certain time t and have since possibly been exchanging genes at migration rates m1 (from unit 2 to unit 1) and m2 (from 1 to 2). The program estimates posterior probability distributions of these three parameters (t, m1 and m2) and additionally the effective population size of the ancestral population (Θ_A) and of the two descendant units (Θ_1 and Θ_2). The program also yields estimates for the number of migration events through time.

Results

<u>Gene diversity</u>

Table 2 shows summary statistics for the nucleotide base composition, transition / transversion bias and percentage sequence divergence. Table 3 shows haplotype and nucleotide diversity, Watterson's θ, Tajima's D and Fu and Li's D for the complete dataset, and for each species.

Table 2 - Nucleotide base composition (A, C, G and T), transition/transversion bias (R), and intra (mar – *T. marmoratus*, and pyg – *T. pygmaeus*) and interspecific percentage sequence divergence (p-distance; ± s.e.) for the four *loci*.

Locus	Nucleotide base composition (%)				R	% Divergence [± s.e.]		
	A	C	G	T		mar	pyg	inter
βfib *int*7	29.7	19.1	18.2	33.1	0.537	0.007 ± 0.002	0.013 ± 0.003	0.014 ± 0.004
Cal *int*C	25.3	17.0	24.5	33.1	1.188	0.004 ± 0.002	0.004 ± 0.001	0.014 ± 0.005
Pdgfr α	28.3	21.2	18.3	32.1	3.364	0.003 ± 0.001	0.002 ± 0.001	0.004 ± 0.002
ND 4	29.4	29.8	14.9	25.9	6.681	0.015 ± 0.002	0.016 ± 0.003	0.038 ± 0.006

Table 3 – Sample size (N), length of fragment (L), haplotype diversity (Hd), nucleotide diversity (π), Theta (θ), and significance of neutrality tests (Tajima's D, and Fu and Li's D for *Triturus marmoratus*, *T. pygmaeus* and the total dataset. ** - significant at α=0.01.

Species	Locus	N	L	Hd	π	θ	D (Tajima)	D (Fu & Li)
Triturus marmoratus	βfib *int7*	111	500	0.607	0.006	0.006	NS	NS
	Cal *intC*	133	472	0.567	0.004	0.006	NS	NS
	Pdgfr α	124	672	0.517	0.002	0.003	NS	NS
	ND 4	160	658	0.886	0.015	0.019	NS	NS
Triturus pygmaeus	βfib *int7*	172	500	0.924	0.013	0.010	NS	NS
	Cal *intC*	198	472	0.743	0.003	0.008	NS	NS
	Pdgfr α	214	672	0.746	0.003	0.003	NS	NS
	ND 4	165	658	0.911	0.016	0.024	NS	- 3.336 **
Total	βfib *int7*	283	500	0.886	0.012	0.010	NS	NS
	Cal *intC*	331	472	0.815	0.009	0.009	NS	- 3.521 **
	Pdgfr α	338	672	0.769	0.003	0.004	NS	NS
	ND 4	325	658	0.933	0.027	0.029	NS	- 4.190 **

mtDNA diversity

The haplotype network for 658 bp of the ND4 gene for 324 individuals from 67 populations shows two clear groups separated by nineteen mutational steps (Figure 2). The first group (M) consists of 35 haplotypes present in 144 samples of *T. marmoratus* and 23 of *T. pygmaeus*. The 39 haplotypes of the second group (P) are present in 16 samples of *T. marmoratus* and 141 of *T. pygmaeus*. The outgroup, *T. cristatus*, connects with the M group at 95 mutational steps from H35, which is in turn four mutational steps away from H32, the M-group haplotype closest to the P-group. Some *T. marmoratus* individuals from Areia, Coimbra, Senhora do Almurtão and Vila Velha de Rodão show P haplotypes, while some *T. pygmaeus* from Casal Palomero, Esperança, Gavião, Mora, Nisa, Palomero, Zebreira and Zebreira West exhibit M haplotypes.

Beta fibrinogen diversity

The beta fibrinogen intron 7 dataset consists of 270 sequences (500 bp), from 208 individuals in 53 populations. The haplotype network shows 65 haplotypes divided into three major groups, separated by 2-4 mutational steps (Figure 3). The M-group of 14 haplotypes consists of 83 *T. marmoratus* samples and 12 *T. pygmaeus*, while the other two groups together represent 156 *T. pygmaeus* and 25 *T. marmoratus* samples.

Calreticulin intron c diversity

We obtained 321 sequences of the intron c of calreticulin (472 bp), from 235 individuals of 56 populations. The haplotype network (Figure 4) presents two distinct groups (M and P) separated by five mutational steps. Six haplotypes forming the M group are present in 115 *T. marmoratus* and 4 *T. pygmaeus*, while the 22 P group haplotypes were found in 18 *T. marmoratus* and 183 *T. pygmaeus*.

Platelet derived growth factor receptor alpha diversity

For Pdgfrα, we obtained 332 sequences from 242 individuals of 56 populations (672 bp). The haplotype network consists of 23 haplotypes (Figure 5). There are two groups of haplotypes (M and P) separated by one mutational step. The M group consists of six haplotypes present in 106 *T. marmoratus* and 21 *T. pygmaeus*, while the P group has 17 haplotypes and is represented by 30 *T. marmoratus* and 175 *T. pygmaeus*.

Mutation rates

Mutation rates were 4.528×10^{-3} subst/site/Ma for the mitochondrial gene ND4, 8.758×10^{-4} subst/site/Ma for βfib*int*7, 1.351×10^{-3} subst/site/Ma for Cal*int*C and 1.13×10^{-3} subst/site/Ma for Pdgfrα. The geometric mean of the substitution rates is 1.568×10^{-3} subst/site/Ma or 0.892 subst/Ma.

Isolation with migration analysis

The IM method assumes that the loci considered have not been subject to recombination or to directional or balancing selection. The null hypothesis of no recombination was not rejected by the phi test in any of the markers and neutrality was rejected for Cal*int*C and ND4 in the combined dataset and for ND4 in *T. pygmaeus* (Table 3).
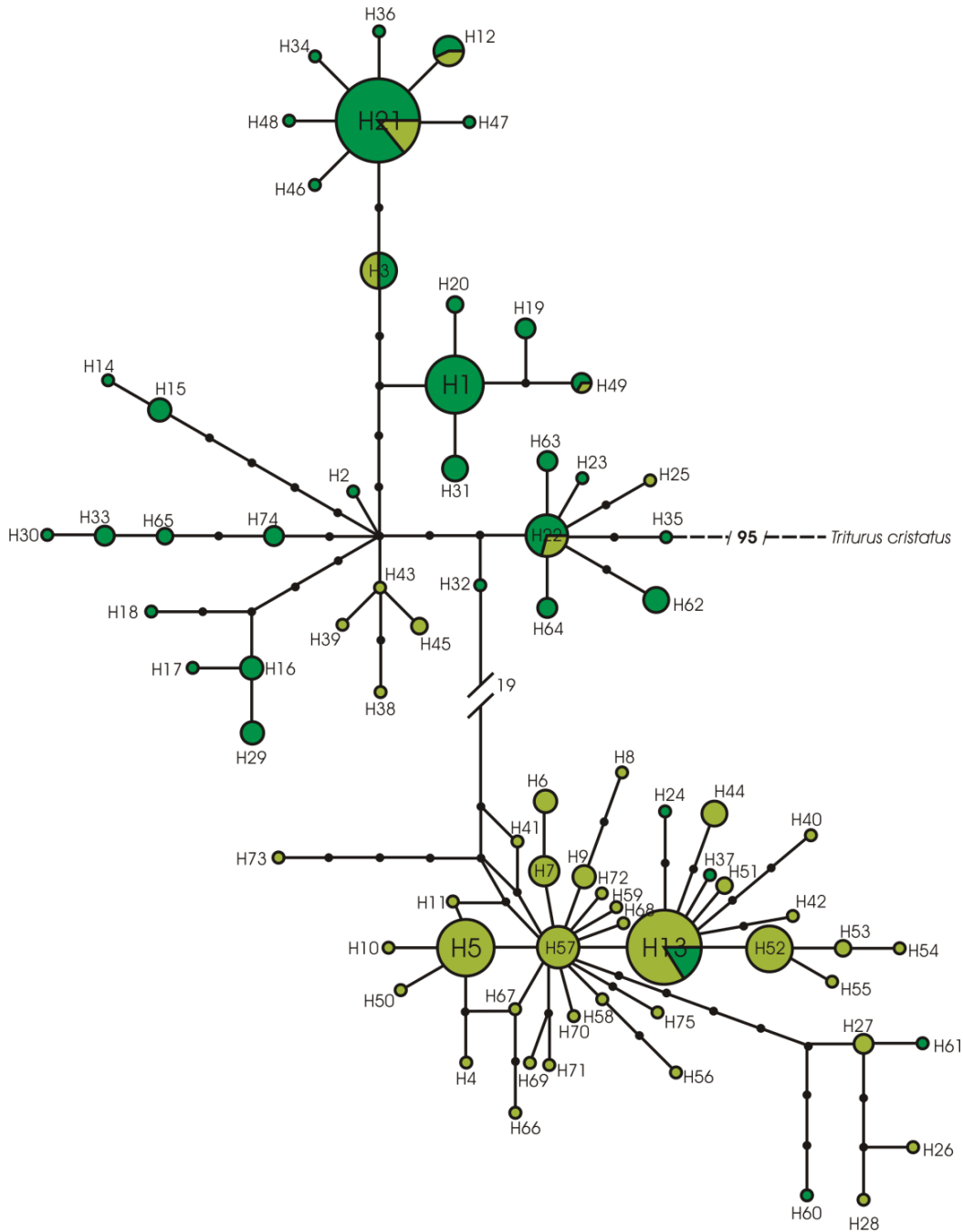
Figure 2 - Haplotype network representing relationship between alleles of the mitochondrial gene ND4 from marbled newts. Size of circles is proportional to frequency of haplotypes. Black circles are missing haplotypes and pie slices represent frequency of the haplotype in *T. marmoratus* (dark colour) and *T. pygmaeus* (light). The number nineteen surrounded by the two slashes in the centre of the figure represents the number of mutations separating the two haplogroups (M and P, see text).
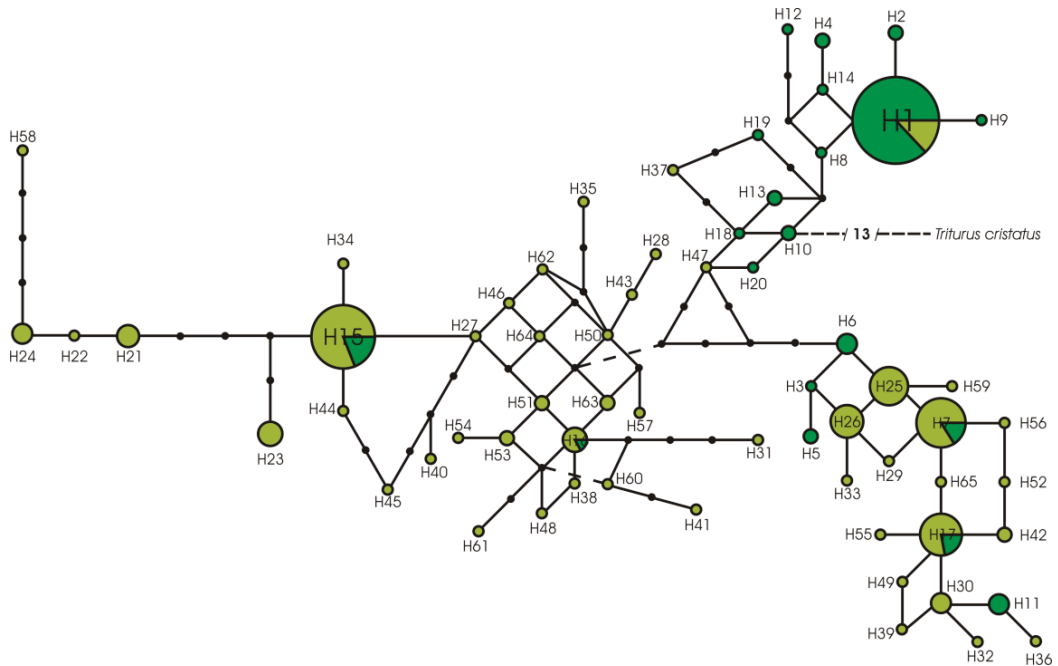
Figure 3 - Haplotype network representing relationship between alleles of the nuclear intron βfib *int*7 from marbled newts**.** Representation follows figure 2. Interrupted line at the centre of the network represents a zero-length connection.
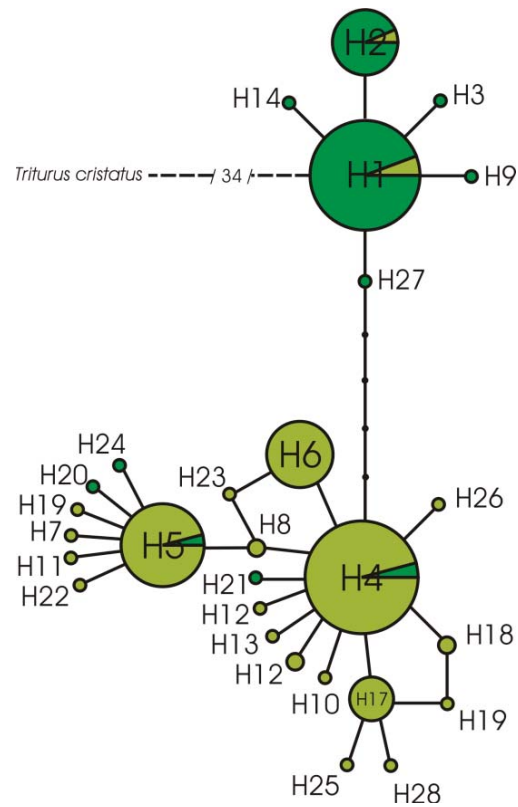

Figure 4 - Haplotype network representing relationship between alleles of the nuclear intron Cal*int*C from marbled newts. Representation follows figure 2.
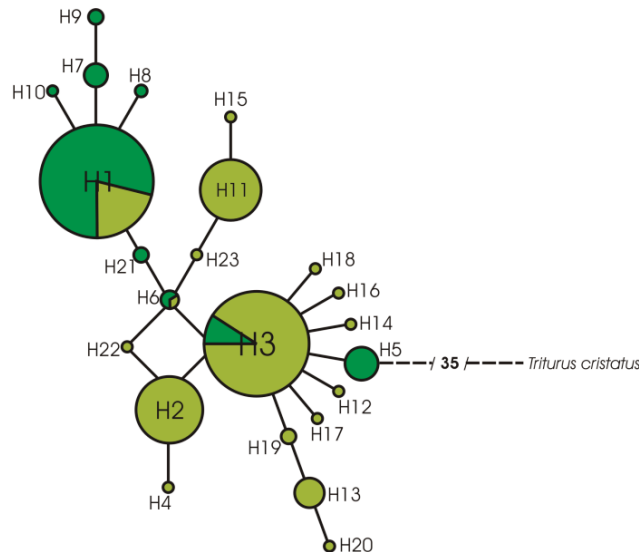
Figure 5 - Haplotype network representing relationship between alleles of the nuclear intron PDGFRα from marbled newts. Representation follows figure 2.

Table 4 summarizes the marginal posterior density curves and maximum likelihood estimates for all parameters in the complete dataset, and the three areas studied. For the ancestral population size and time of divergence, flat curves of the marginal posterior densities without distinct peaks indicate that these parameters could not be reliably estimated from our data. In Table 5, we present the conversion of parameter estimates to demographic quantities.

Table 4 - Results of IMa analysis with effective population size for *T. marmoratus* (q1), *T. pygmaeus* (q2) and the ancestral population (qa), migration rate from *T. pygmaeus* to *T. marmoratus* (m1 migration rate from *T. marmoratus* to *T. pygmaeus* (m2) and the divergence time between them (t).

	$\Theta 1$	95% CI	$\Theta 2$	95% CI	Θa	95% CI
Coastal	4.321	2.967 - 6.716	7.341	5.362 - 10.256	3.593	0.885 - 88.563
Tejo	1.287	0.585 - 2.833	3.629	1.944 - 7.235	4.987	1.194 - 45.402
Idanha	0.712	0.289 - 2.138	2.562	1.329 - 5.528	8.533	1.483 - 37.351

	m1	95% CI	*m2*	95% CI	*t*	95% CI
Coastal	0.206	0.085 - 0.482	0.001	0.001 - 0.086	2.78	1.74 - 23.18
Tejo	1.625	0.755 - 7.435	0.675	0.205 - 3.685	1.42	1.18 - 37.86
Idanha	0.755	0.385 - 8.825	0.235	0.055 - 2.605	1.26	0.70 - 37.42

Table 5 – Conversion of parameter estimates in Table 4 to demographic quantities.

	N1	N2	Na	2N1m1	2N2m2	t
Coastal	106 364	180 692	88 424	0.444	0.002	1 094 806
Tejo	28 433	86 834	148 308	0.973	1.173	118 144
Idanha	10 746	67 643	187 754	0.180	0.378	527 712

Chapter 6 – Variable gene flow along a newt contact zone

Coastal area

Dispersal estimates (2Nm) in the coastal area (Table 4) show near-zero (0.002) migration from *T. marmoratus* to *T. pygmaeus* (the hypothesis of *m2* = 0 was not rejected in an analysis of nested models), and migration significantly different from zero (0.444) in the opposite direction (*m1* = 0 was rejected at p<0.05). Other nested models that are not rejected involve equal values for effective population sizes. Estimated time of divergence shows a distinct peak at approximately 1 094 806 years with a large confidence interval. Effective population (*Ne*) sizes are 106 364 for *T. marmoratus*, 180 692 for *T. pygmaeus* and 88 424 for the ancestral population.

Tejo basin

Migration estimates in both directions are significantly different from zero, with similar migration rates (0.973 vs. 1.173). Examination of nested models of migration rejects models with m1 or m2 = 0, but not models with m1=m2. The estimated time of divergence is 118 144 years. Effective population sizes are estimated at 28 433 for *T. marmoratus*, 86 834 for *T. pygmaeus* and 148 308 for the ancestral population.

Idanha

Migration rates in Idanha are significantly different from zero in both directions. Estimates of migration rates are *m1* = 0.180 and *m2* = 0.378. Examination of nested models of migration show the rejection of models where *m1* and/or *m2* = 0, but not of models with *m1=m2*. Estimated time of divergence is 527 712 years. Effective population sizes are 10 746 for *T. marmoratus*, 67 643 for *T. pygmaeus* and 187 754 for the ancestral population.

Migration over time

Figure 6 shows the distribution of migration events backwards in time in the three areas. Migration takes off at around the same time for the three areas (2.5 Ma). In the coastal area, a plateau is reached around 1.1 Ma followed by an increase of migration in the last 100 ka (thousand years) for m1, while m2 is zero. In the Tejo Basin, migration is the highest until ca. 500 ka when it reduces to similar levels than the other areas. m1 is consistently higher than m2, but the difference is not significant. In Idanha, there is a gradual increase of migration until it reaches a plateau around 600 ka that is maintained until very recently, with m1 consistently higher than m2, but the difference is not significant.

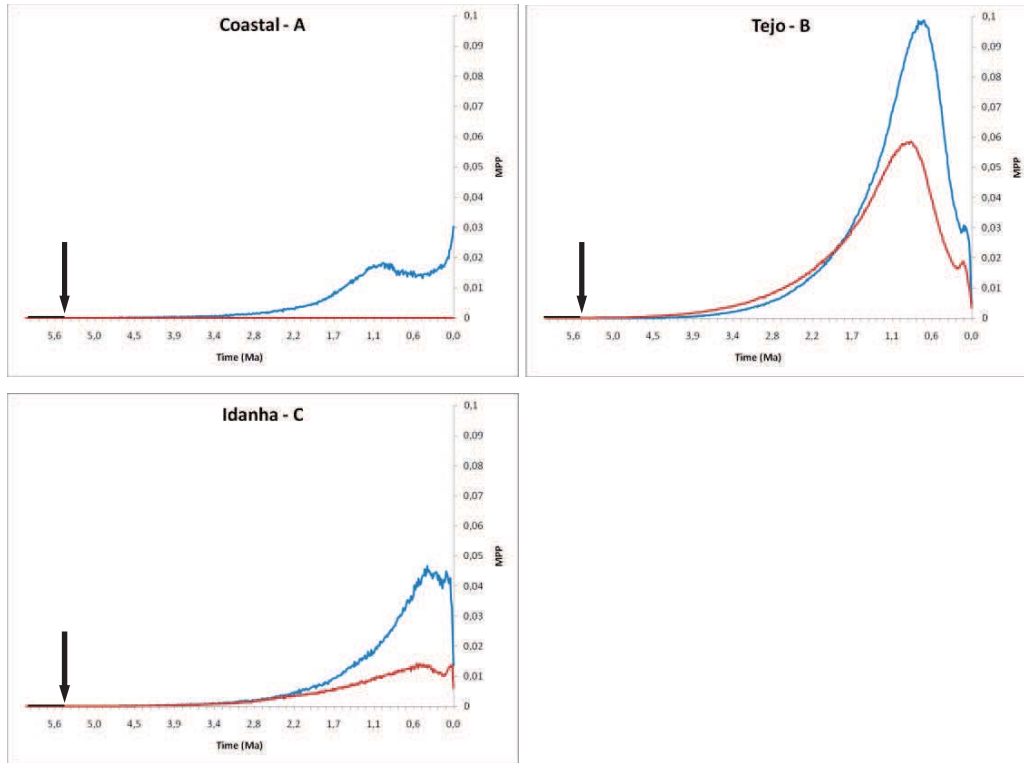**Figure 6** - Temporal distribution of migration times in the three study areas. The horizontal axis indicates time in millions of years (Ma) and the vertical axis denotes marginal posterior probability (MPP). Blue curve indicates *m1* (migration from *T. pygmaeus* to *T. marmoratus*) and red line *m2* (migration in the opposite direction). In the coastal region m2 is not significantly different from zero and hence represented by a straight line. Arrows indicate divergence time based on mtDNA (5.4 Ma; Arntzen *et al.*, 2007).

Discussion

Species divergence and reticulation, assumptions of the method

The estimated time of divergence between *T. pygmaeus* and *T. marmoratus* has large confidence intervals, with a 95% upper bound of the confidence interval of ca. 10 Ma for the coastal region. A phylogenetic analysis of mtDNA estimated that the two species separated around 5.4 ± 2.2 Ma (ARNTZEN *et al.*, 2007). The order in which the interspecific contact was established is estimated as A (Coastal), B (Tejo) and then C (Idanha). Given the large uncertainty we will refrain from making temporal inferences in an absolute sense.

One assumption of IMa is that there are no populations more closely related to the studied populations than the two sampled populations are to one another (Nielsen and Wakeley, 2001). We believe that breaking the assumption will not affect the

results, as in interspecific datasets the genetic substructure within the species is significantly less than between them.

Hybrid zone position and width

Ample evidence suggests that the position of a hybrid zone may be determined by ecological conditions. At smaller scale, also the width of the zone may be affected, suggesting levels of dispersal across the zone to vary with the environment. We studied interspecific gene flow across a newt hybrid zone in Portugal and Spain, for which we selected four areas representing different environmental settings and with different predictions on gene flow. Moreover, in non-equilibrium conditions such as we reconstructed in the coastal area of Portugal where the newt *T. pygmaeus* has been superseding its sister species *T. marmoratus*, gene flow is predicted to be asymmetric. The estimates of dispersal rates and symmetry are indeed different in three out of four selected study areas (data on one area are as yet incomplete).

According to theory, a tension hybrid zone will become fixed in a place such that its length is minimized (BARTON and HEWITT, 1995). Such a situation we encountered at Idanha with no obvious ecological parameter associated to the zone's position other than the Tejo river at ca. 50 km to the southwest and the western fringe of the Central System mountain range at ca. 100 km to the east (CHAPTER 8). The amount of gene flow was expected to be higher here, with no physical barrier, than at either side, with riverine and mountain barriers, respectively, but this was not confirmed by the results. The time plot of migration events, however, shows that the *current* level of gene flow for Tejo and Idanha is similar (Figure 6; no data for area D yet). The origin of the Tejo at its present position started with the lifting of the area and the subsequent incision by the Tejo of its own depositions at the Middle Pliocene, with a second lifting phase at the Late Pliocene (G.-J. Vis, pers. comm.). This would suggest gene flow between the species to be unhampered by the river up to ca. 2 Ma before present. More gene flow between populations at either side of the river then at present may also have been possible in periods of decreased fluvial discharge during periods of climate change in the Pleistocene.

A similar situation was observed in two species of chorus frogs (*Pseudacris ferarium / P. triseriata*) with a hybrid zone at the Ohio basin, USA. The frog species formation is not related to the Ohio river (that is more recent than the frogs) but to

another river more to the north that disappeared in the Middle Pleistocene (Lemmon *et al.*, 2007).

We have reported the mosaic distribution of *T. marmoratus* and *T. pygmaeus* western Portugal, including an isolated patch of *T. marmoratus* near Caldas da Rainha that is characterized by a higher prevalence of terrain used for orchards than the surrounding terrain (Figure 1A; see CHAPTER 9). A straightforward explanation for such a pattern, at least in organisms with low dispersal capability such as amphibians, is the superseding by one species (*T. pygmaeus*) of the other (*T. marmoratus*). The near-absence of genetic footprints of *T. marmoratus* in the areas that changed species occupancy further indicates that the process did not involve much hybridization, while the peculiar distribution pattern of *T. pygmaeus* suggest that the advance has been particularly prominent over the dunal systems of coastal Portugal. With no barrier in place other than the newly reached one at the Vouga estuary in Aveiro, the advance may have been fast and relatively recent. It is therewith interesting to note that the temporal profile of gene-flow shows a recent increase, different from the pattern observed in the other study areas (Fig. 6).

A common feature among the three transects studied so far is the higher level of gene-flow from *T. pygmaeus* into *T. marmoratus* than the other way round (although the difference is only statistically significant in the coastal area). This observation is in line with a general, historical northward advance of *T. pygmaeus*, not stopped by *T. marmoratus*, but by barriers posed by the environment such as the mountains of the Central System in Spain, the river Tejo in central Portugal and also, perhaps more recently, the Vouga estuary at the Atlantic coast. A principal difference between the species is the higher general population size of *T. pygmaeus* than in *T. marmoratus*. This is expressed through generally larger population sizes and denser networks of *T. pygmaeus* than in *T. marmoratus* (unpublished field observations). It is also expressed by the effective population sizes estimates that are consistently higher for *T. pygmaeus* than in *T. marmoratus* (Tables 5 and 6). Typical breeding sites are large and temporary ponds for *T. pygmaeus* and smaller, more permanent ponds, tanks and wells for *T. marmoratus* (CHAPTER 8) that may be more widely distributed over lowland and mountainous terrain, respectively. We predict the northward advance of *T. pygmaeus* to be continued once the riverine barriers of Tejo and Vouga have been taken. Ecogeographical models suggest that in central Portugal the zone will find a

stable position at ca. 40 km to the north (CHAPTER 8). Along the coast there may not be any impediment other than the absence of coastal dunes.

Acknowledgments

References

ALEXANDRINO, J., FROUFE, E. , ARNTZEN, J. W. and FERRAND, N. (2000) Genetic subdivision, glacial refugia and postglacial recolonization in the golden-striped salamander, *Chioglossa lusitanica* (Amphibia : Urodela). *Molecular Ecology* **9**, 771-781.

ARNOLD, M.L. (1992) Natural hybridization as an evolutionary process. *Annual Review of Ecology and Systematics* **23**, 237-261.

ARNTZEN, J. W. (1978) Some hypotheses on postglacial migrations of the Fire-bellied Toad, *Bombina bombina* (Linnaeus) and the Yellow-bellied Toad, *Bombina variegata* (Linnaeus). *Journal Biogeography* **5**, 339-345.

ARNTZEN, J. W. (1996) Parameters of ecology and scale integrate the gradient and mosaic models of hybrid zone structure in *Bombina* toads and *Triturus* newts. *Israel Journal of Zoology* **42**, 111-119.

ARNTZEN, J. W. and WALLIS, G. P. (1991) Restricted gene flow in a moving hybrid zone of the newts *Triturus cristatus* and *T. marmoratus* in western France. *Evolution* **45**, 805-826.

BANDELT, H.-J., FORSTER P. and RÖHL A. (1999) Median-joining networks for inferring intraspecific phylogenies. *Molecular Biology and Evolution* **16**, 37-48.

BARTON, N. H. and HEWITT, G. M. (1985) Analysis of Hybrid Zones. *Annual Review of Ecology and Systematics* **16**, 113-148.

BOŽÍKOVÁ, E., MUNCLINGER, P., TEETER, K. C., TUCKER, P. K., MACHOLÁN, M. and PIÁLEK, J. (2005) Mitochondrial DNA in the hybrid zone between *Mus musculus musculus* and *Mus musculus domesticus*: a comparison of two transects. *Biological Journal of the Linnean Society* **84**, 363-378.

BRUEN, T.C., PHILIPPE H. and BRYANT D. (2006) A simple and robust statistical test for detecting the presence of recombination. *Genetics* **172**, 2665-2681.

CAETANO, M. H. and CASTANET, J. (1993) Variability and microevolutionary patterns in *Triturus marmoratus* from Portugal: age, size, longevity and individual growth *Amphibia-Reptilia* **14**, 117-129.

CASTELLA, V., RUEDI, M., EXCOFFIER, L., IBÁÑEZ, C., ARLETTAZ, R. and HAUSSER, J. (2000) Is the Gibraltar Strait a barrier to gene flow for the bat *Myotis myotis* (Chiroptera: Vespertilionidae)? *Molecular Ecology* **9**, 1761-1772.

COSTA, J. C., AGUIAR C., CAPELO J. H., LOUSÃ M. and NETO C. (1998) Biogeografia de Portugal continental. *Quercetea* **1**, 5–56.

COYNE, J. A. and ORR, H. A. (2004) *Speciation*. Sinauer Associates, Inc., Sunderland, MA.

DASMAHAPATRA, K. K., BLUM, M. J., AIELLO, A., HACKWELL, S., DAVIES, N., BERMINGHAM, E. P. and MALLET, J. (2002) Inferences from a rapidly moving hybrid zone. *Evolution* **56**, 741-753.

DIAZ-PANÍAGUA, C., MATEO, J. A. and ANDREU, A. C. (1996) Age and size structure of populations of small marbled newts (*Triturus marmoratus pygmaeus*) from Doñana National Park (SW Spain). A case of dwarfism among dwarfs. *Journal of Zoology* **239**, 83-92.

DRUMMOND, A.J. and RAMBAUT A. (2007) BEAST: Bayesian evolutionary analysis by sampling trees. *BMC Evolutionary Biology* **7**: 214.

BENJAMIN M. FITZPATRICK, H. BRADLEY SHAFFER, G. WALLIS (2004) Environment-dependent admixture dynamics in a tiger salamander hybrid zone *Evolution* **58**, 1282-1293.

FRANCILLON-VIEILLOT, H., ARNTZEN, J. W. and GÉRAUDIE, J. (1990) Age, growth and longevity of sympatric *Triturus cristatus*, *T. marmoratus* and their hybrids (Amphibia, Urodela): a skeletochronological comparison. *Journal of Herpetology* **24**, 13-22.

GARCÍA-PARÍS, M., ALCOBENDAS, M. and ALBERCH, P. (1998) Influence of the Guadalquivir River Basin on mitochondrial DNA evolution of *Salamandra salamandra* (Caudata: Salamandridae) from southern Spain. *Copeia* **1998,** 173-176.

GARCÍA-PARÍS, M., ARANO B. and HERRERO P. (2001) Molecular Characterization of the contact zone between *Triturus pygmaeus* and *T. marmoratus* (Caudata:

Salamandridae) in Central Spain and their taxonomic assessment. *Revista Española de Herpetología* **15**, 115-126.

GASCON, C. (1996) Amphibian litter fauna and river barriers in flooded and non-flooded Amazonian rain forest. *Biotropica* **28**, 136-140

HALL, T.A. (1999) BioEdit: a user-friendly biological sequence alignment editor and analysis program for Windows 95/98/NT. *Nucleic Acids Symposium Series* **41**, 95-98.

HEY, J. and NIELSEN R. (2004) Multilocus methods for estimating population sizes, migration rates and divergence time, with applications to the divergence of *Drosophila pseudoobscura* and *D. persimilis*. *Genetics* **167**, 747-760.

HAYES, F. E. and SEWLAL, J. N. (2004) The Amazon River as a dispersal barrier to passerine birds: effects of river width, habitat and taxonomy. *Journal of Biogeography* **31**, 1809-1818.

JAKOB, C., MIAUD, C., CRIVELLI, A. J. and VEITH, M. (2003) How to cope with periods of drought? Age at maturity, longevity, and growth of marbled newts (*Triturus marmoratus*) in Mediterranean temporary ponds. *Canadian Journal of Zoology* **81**, 1905-1911.

JEHLE, R., ARNTZEN J.W., BURKE T., KRUPA P. and HÖDL W. (2001) The annual number of breeding adults and the effective population size of syntopic newts (*Triturus cristatus*, *T. marmoratus*). *Molecular Ecology* **10**, 839-850.

JIGGINS, C. D. and MALLET, J. (2000) Bimodal hybrid zones and speciation *Trends in Ecology and Evolution* **15**, 250-255.

KEY, K. H. L. (1968) The concept of stasipatric speciation. *Systematic Zoology* **17**, 14-22.

KRUUK, L. E. B., BAIRD, S. J. E., GALE, K. S., BARTON, N. H. (1999) A comparison of multilocus clines maintained by environmental adaptation or by selection against hybrids *Genetics*, **153**, 1959-1971.

LEMMON, E. M., LEMMON, A. R. and CANNATELLA, D. C. (2007) Geological and climatic forces driving speciation in the continentally distributed trilling chorus frogs (*Pseudacris*). *Evolution* **61,** 2086-2103.

LOUREIRO, A., FERRAND DE ALMEIDA N., CARRETERO M.A. and PAULO O.S. (2008) *Atlas dos Anfíbios e Répteis de Portugal* Instituto da Conservação da Natureza e da Biodiversidade, Lisboa.

MacCallum, C. J., Nurnberger, B., Barton, N. H. and Szymura, J. M. (1998) Habitat preference in the *Bombina* hybrid zone in Croatia. *Evolution* **52**, 227-239.

Nielsen, R. and, Wakeley, J. (2001) Distinguishing migration from isolation: a Markov Chain Monte Carlo approach. *Genetics* **158**, 885-896.

Pearson, S. F. (2000) Behavioral asymmetries in a moving hybrid zone. *Behavioral Ecology* **11**, 84-92.

Posada, D. and Crandall K.A. (2001) Intraspecific gene genealogies: trees grafting into networks. *Trends in Ecology and Evolution* **16**, 37-45.

Rand, D. M. and Harrison, R. G. (1989) Ecological genetics of a mosaic hybrid zone: mitochondrial, nuclear, and reproductive differentiation of crickets by soil type. *Evolution* **43,** 432-449.

Rozas, J., Sanchez-DelBarrio J.C., Messeguer X. and Rozas R. (2003) DnaSP, DNA polymorphism analyses by the coalescent and other methods. *Bioinformatics* **19**, 2496-2497.

Sequeira, F., Alexandrino, J., Rocha, S., Arntzen, J. W. and Ferrand, N. (2005) Genetic exchange across a hybrid zone within the Iberian endemic golden-striped salamander, *Chioglossa lusitanica. Molecular Ecology*, **14**, 245-254.

Slatkin, M. (1985) Gene flow in natural populations. *Annual Review of Ecology and Systematics* **16**, 393-430.

Slechtova, V., Bohlen, J., Freyhof, J., Persta, H. and Delmastro, G. B. (2004) The Alps as barrier to dispersal in cold-adapted freshwater fishes? Phylogeographic history and taxonomic status of the bullhead in the Adriatic freshwater drainage. *Molecular Phylogenetics and Evolution* **33**, 225-239.

Steinfartz, S., Vicario S., Arntzen J.W. and Caccone A. (2007) A Bayesian approach on molecules and behavior: reconsidering phylogenetic and evolutionary patterns of the Salamandridae with emphasis on *Triturus* newts. *Journal of Experimental Zoology Part B: Molecular and Developmental Evolution* **308B**, 139-162.

Stephens, M., Smith N.J. and Donnelly P. (2001) A new statistical method for haplotype reconstruction from population data. *The American Journal of Human Genetics* **68**, 978-989.

SZYMURA, J. M. (1993) Analysis of hybrid zones with *Bombina*. in *Hybrid zones and the evolutionary process* (eds. HARRISON, R. G.). Oxford University Press, New York.

SZYMURA, J. M. and BARTON, N. H. (1991) The genetic structure of the hybrid zone between the fire-bellied toads *Bombina bombina* and *B. variegata*: comparisons between transects and between loci. *Evolution* **45**, 237-261.

TAMURA, K., DUDLEY J., NEI M. and KUMAR S. (2007) MEGA4: Molecular Evolutionary Genetics Analysis (MEGA) Software Version 4.0. *Molecular Biology and Evolution* **24**, 1596-1599.

YANCHUKOV, A., HOFMAN, S., SZYMURA, J. M., MEZHZHERIN, S. V., MOROZOV-LEONOV, S. Y., BARTON, N. H., NURNBERGER, B. and HARRISON, R. (2006) Hybridization of *Bombina bombina* and *B. variegata* (Anura, Discoglossidae) at a sharp ecotone in western Ukraine: comparisons across transects and over time. *Evolution* **60**, 583-600.